analytical chemistry

ARTICLE

pubs.acs.org/ac

Structural Characterization of Individual Vesicles using Fluorescence Microscopy

Emily C. Heider, Moussa Barhoum, Kyle Edwards, Karl-Heinz Gericke,[†] and Joel M. Harris*

Department of Chemistry, University of Utah, 315 South 1400 East, Salt Lake City, Utah 84112-0850, United States

ABSTRACT: Extrusion of hydrated lipid suspensions is frequently employed to produce vesicles of uniform size, and the resulting vesicles are often reported to be unilamellar. We describe a method for the quantitative fluorescence image analysis of individual vesicles to obtain information on the size, lamellarity, and structure of vesicles produced by extrusion. In contrast to methods for bulk analysis, fluorescence microscopy provides information about individual vesicles, rather than averaged results, and heterogeneities in vesicle populations can be characterized. Phosphatidylcholine vesicles containing small fractions of biotin-modified phospholipid and fluorescently labeled 7-nitro-2,1,3-benzoxadiazol-4-yl (NBD) phospholipid were immobilized through biotin−avidin−biotin binding to the surface of a biotin-modified glass coverslip. Biotin was attached to the surface in a mixed cyano-terminated silane monolayer. Initial fluorescence intensities for each immobilized vesicle were recorded, and a solution of membrane impermeable quencher was passed through the flow cell to quench the fluorescence of the outer layer. Fluorescence from individual vesicles was measured by fitting the spots to 2-dimensional Gaussian functions. The integrated signals under the peaks yielded a pre- and postquench intensity. From the fractional loss of intensity, the number and structure of the bilayers in individual vesicles could be quantified; the results showed that extruded vesicles exhibit a distribution of size, lamellarity, and structure.

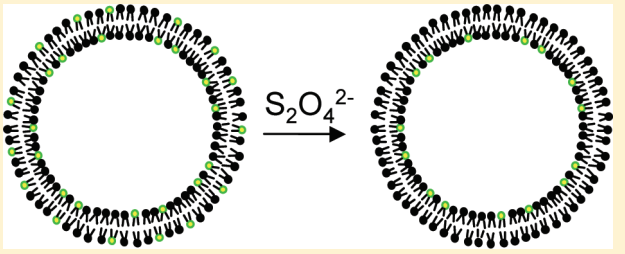

Phospholipid vesicles (liposomes) are used in a variety of applications in chemical analysis including the formation of pseudostationary phases[1] or bilayer coatings on solid supports for separations,[2,3] encapsulation carriers for pharmaceuticals,[4−6] vessels for isolating chemical reactions in small volumes,[7−10] and platforms for analytical reagents assays and sensing.[11−13] Several methods are reported to produce vesicles with uniform size and number of bilayers (lamellarity) for these applications.[14−19] Extrusion of hydrated lipid suspensions through small pores is often employed for this purpose, through the use of a manual, syringe-based extrusion apparatus introduced by McDonald et al.[20] The structure of extruded phospholipid vesicles smaller than 400 nm have been studied extensively,[17,21,22] but vesicles of larger size (0.5−1 μm) are of considerable interest because their size facilitates examination of membrane structure,[23] they are conducive to study of their contents using optical microscopy,[24−26] and encapsulation of components for reactions in small volumes.[7,10,27]

Many methods have been reported for the quantitative analysis of vesicle size and structure, and these techniques have been used to evaluate a range of vesicle preparation procedures. Some bulk methods of analysis include NMR,[15,17] small-angle neutron scattering,[21] dynamic light scattering,[28] and fluorescence quenching.[29] These methods suffer from the disadvantage that the information obtained is averaged over the vesicle population and details about individual structures and population heterogeneities are not available. Analysis of individual vesicles has been accomplished using methods such as flow cytometry,[30] cryoelectron microscopy,[15,28] two-photon microscopy,[31] confocal laser scanning microscopy,[32] and phase contrast microscopy.[16] Of these techniques, flow cytometry is best-suited to analyzing a large population of vesicles, but suffers the disadvantage that large vesicles and vesicle aggregates are not readily distinguished;[33] the method also uses solid beads as calibration standards, whose refractive index differs from that of the vesicles to which their scattering is compared.[34] In recent work by Lohr and co-workers,[35] epi-illumination fluorescence microscopy was used to measure the fluorescence intensity distributions of individual, 100- and 200-nm vesicles prepared with a fluorescent label. Images were thresholded to find spots, and the total intensities of spots were assumed to be proportional to total lipid bilayer area. The conversion between intensity and the vesicle size was made by using dynamic light scattering of the vesicle population to calibrate the average fluorescence response. This analysis can be in error if vesicles are multilamellar, where more intense fluorescence arising from multiple bilayers would be misinterpreted as larger sized vesicles. To test for multilamellarity, a fluorescence quenching analysis on the vesicle population showed that the multilamellar fraction of the 100- and 200-nm vesicle samples was ~5 and 10%, respectively,[35] so total intensity should be relatively accurate measure of size for these smaller vesicles. For larger vesicles, where a much greater

Received: March 11, 2011
Accepted: May 3, 2011
Published: May 16, 2011

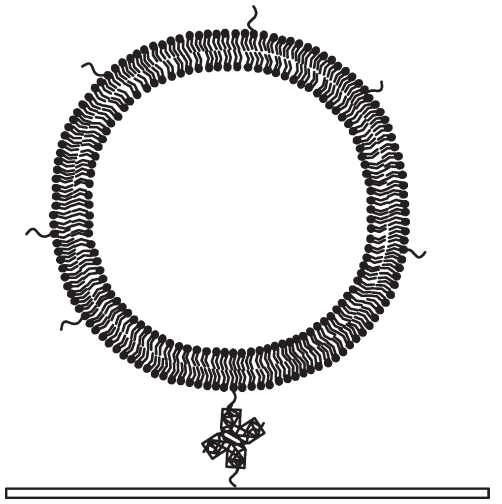

Figure 1. Illustration of a biotin−avidin−biotin immobilized vesicle. Biotin extends from the coverslide-modified amine-cyano monolayer via a PEO_4 linkage. Avidin on the coverslide surface is conjugated both to the biotin on the surface as well as the biotinyl-PE lipid incorporated into the phospholipid vesicle.

fraction of multilamellar structures is expected,[29] a different strategy of analysis is required.

In the present work, we describe a fluorescence imaging method to measure simultaneously both size and lamellarity of individual extruded vesicles in the range of 0.5−2-μm diameter. Data are reported on the distributions of size and lamellarity of the extruded 1,2-dipalmitoyl-sn-glycero-3-phosphocholine (DPPC) vesicles. Vesicles were fluorescently labeled by including a small fraction (0.5%) of lipid with a headgroup attached fluorescent probe, *N*-(7-nitrobenz-2-oxa-1,3-diazol-4-yl)-1, 2-dihexadecanoyl-sn-glycero-3-phosphoethanolamine (NBD-PE). To determine the lamellarity, the membrane impermeable anion, dithionite ($S_2O_4^{2-}$) which is in equilibrium with the SO^{2-} radical in aqueous solution,[36] was used to reduce the nitro group of NBD to an amine.[29] This reduction quenches the fluorescence on the outer vesicle layer while leaving the internal NBD-PE unreacted. Acquiring epi-illumination fluorescence microscopy images of the labeled vesicles before and after quenching allows quantification of the fractional loss of fluorescence intensity, and reports the lamellarity of individual vesicles in an image.

The vesicles were immobilized, to withstand the flow of the quenching solution, by including small fractions of biotin-modified phospholipid in addition to fluorescent NBD-PE in the DPPC vesicles. The biotinylated vesicles were immobilized through a biotin−avidin-biotin interaction to the surface of a biotin-modified glass coverslip. Biotin was attached to the surface in a mixed amine-cyano monolayer[37] by reaction of amine binding sites with *N*-hydroxysuccinimide ester-PEO_4-biotin, which was conjugated with avidin and used to capture the biotinylated vesicles, analogous to previous vesicle immobilization procedures using biotinylated planar-lipid bilayers on glass or biotinylated *n*-alkanethiols on gold for a capture surface;[9,35,38,39] see Figure 1. The fluorescence images were analyzed by fitting the vesicle spots to 2-dimensional Gaussian functions and the intensities measured as the integrated signal under the fitted peak. The sizes were corrected for diffraction-limited resolution of the microscope by deconvolution of the point-spread function of the microscope, determined by imaging dye-labeled nanospheres. The results show that extruded DPPC vesicles exhibit a distribution of size and lamellarity.

EXPERIMENTAL SECTION

Reagents and Materials. DPPC, 1,2-dipalmitoyl-sn-glycero-3-phosphoethanolamine-*N*-(biotinyl) (sodium salt) (biotinyl-PE) and a mini-extruder apparatus were obtained from Avanti Polar Lipids, Inc. (Alabaster, AL). NBD-PE and avidin were purchased from Invitrogen Corp. (Carlsbad, CA). NHS-PEG_4-biotin was acquired from Thermo Fisher Scientific (Rockford, IL). (3-aminopropyl)triethoxysilane (APTES) and (2-cyanoethyl)triethoxysilane) (CETES) were purchased from Gelest (Morrisville, PA). Spectrophotometric grade toluene, *n*-heptane, DMF, chloroform, and methanol were from Fisher Scientific (Hampton, NH). Toluene and *n*-heptane were dried over sodium and filtered through Millipore PTFE 0.2-μm filter prior to use (VWR, West Chester, PA). Buffer components tris-(hydroxymethyl)aminomethane (Tris) and $CaCl_2 \cdot H_2O$ were purchased from Mallinckrodt (Paris, KY). Buffers were prepared using quartz-distilled water that was filtered using a Barnstead NANOpure II filter (Boston, MA) with 18 MΩ-cm resistivity. Polycarbonate membranes were produced by Nucleopore (Pleasanton, CA). Glass coverslips (No. 1, 22 × 22 mm) were purchased from VWR (West Chester, PA).

Vesicle Preparation. Unlabeled DPPC vesicles were prepared by removing the chloroform from 200 μL of lipid solution containing 5 mg/mL DPPC by evaporation under nitrogen, followed by 2 h under vacuum. To produce NBD-labeled vesicles, NBD-PE was dissolved in chloroform and a volume sufficient to produce 0.5 mol percent NBD-PE solution was added to the DPPC prior to drying. Biotinylated vesicles were prepared by including fifteen mole percent biotinyl-PE in chloroform with the NBD-PE and DPPC prior to removal of solvent. The dry lipid films were hydrated with 1 mL of buffer containing 50-mM Tris and 10-mM $CaCl_2$, pH 8. Hydrated lipid vesicles were heated to 60 °C for 1 h and then extruded 11 times through 1 μm-diameter polycarbonate filters. Following extrusion, 100 μL of extruded vesicle solution was diluted into 6 mL of buffer.

A population of predominantly unilamellar vesicles was also prepared according to the procedure described by Mayer et al.,[22] in which repeated (5 times) freeze−thaw treatment of hydrated lipids preceded extrusion through two-stacked 100-nm pore membranes. This method was employed using the DPPC/NBD-PE/biotinyl-PE (84.5/0.5/15 mol %) lipid composition as prepared above and the resulting extruded vesicles were diluted 50 μL to 5 mL.

Surface Derivatization. The procedure used to derivatize the surface was a modification of a previous description.[37] The glass coverslips were first cleaned by rinsing in methanol, and then UV-ozone cleaned for 25 min per side (Jelight Co. Model 342). Stock solutions of CETES and APTES were prepared in dry toluene and diluted into one solution with final concentrations of 2-mM CETES and 0.2-mM APTES in dry *n*-heptane. The clean coverslips were immersed with stirring in this solution and reacted for two hours before rinsing twice with toluene and four times with methanol to remove unreacted starting material. The slides were annealed in an oven at 120 °C for 30 min and stored for up to a week in dry methanol.

The amine sites of the modified coverslips were reacted for one hour in 7.5 μM NHS-PEG_4-biotin in DMF using succinimidyl ester binding chemistry to yield biotin extended into

solution, attached to the surface through a PEG chain via an amide bond.[40,41] The slides were again rinsed, twice with DMF and four times with methanol. Finally, 0.15-nM Avidin was prepared in 20-mM phosphate buffer (ionic strength 100 mM with NaCl) at pH 7.5, and the immersion of the glass coverslip in this solution resulted in the attachment of avidin to the surface via hydrogen bonding to biotin. This surface was used to immobilize vesicles prepared with biotinyl-PE.

Fluorimeter Measurements. A Fluorolog fluorescence spectrometer (Horiba Scientific) with 450 W Xe lamp source was used to acquire fluorescence emission from vesicles in bulk solution before and after their quenching with sodium dithionite. For these measurements, 3 mL of the diluted vesicle extrusion were illuminated at 470 nm and their fluorescence emission monitored at 540 nm for 30 s. The sodium dithionite quencher was added (150 μL of 1 M $Na_2S_2O_4$ in 1 M Tris pH 10), and the resulting decrease in fluorescence intensity was monitored over several minutes.

Microscopy Measurements. Immobilized vesicles were imaged using a epi-illumination fluorescence microscope that was slightly modified relative to a previous description.[42] Briefly, the Lexel Model 95 argon ion laser source was tuned to emit a 488-nm line that was passed through a Pellin-Broca prism. The beam was selectively blocked with a Uniblitz electronic shutter, and then was diffused to an incoherent spot after impinging on a rotating, roughened glass disk. A camera lens with 55-mm focal length (f/1.2) reimaged the spot. The band-pass excitation filter (D480/30, Chroma), and a long pass dichroic beam splitter (505dclp, Chroma), filtered the excitation before filling the objective, an oil-immersion Nikon Plan Fluor 100×, 1.3 numerical aperture (N.A.), with 0.2-mm working distance. The objective lens collected the fluorescence emitted by the sample, which was filtered through a long pass dichroic beam splitter and a 510-nm long pass emission filter (HQ510lp, Chroma). The CCD was a Photometrics CoolSNAP HQ (1392 × 1040 imaging array with 6.45 × 6.45 μm pixels). Metamorph Imaging software (Universal Imaging) controlled the CCD (200 ms integration times) and the shutter.

To determine the point spread function of the microscope, 65-nm TAMRA-labeled polystyrene beads (preparation described elsewhere[43]) were deposited onto a glass coverslip at low densities. Using the procedure outlined below for determining size and intensity, the Gaussian-shaped point spread function was measured to have a full-width at half-maximum of 280 nm, which is close to the expected fwhm = 0.72λ/N.A. of 300 nm, for the 1.3 N.A. objective, and emission maxima of 540 nm.

Imaging Individual Vesicles in Parallel. The avidin-modified glass coverslips were placed in a flow cell and imaged for background correction before the biotinylated NBD-labeled vesicles were flushed into the flow cell. After waiting for the vesicles to bind to the surface (approximately one hour) several milliliters of Tris buffer was flushed through the flow cell to remove unbound vesicles. The immobilized vesicles were imaged, and then 1 mL of 1-M $Na_2S_2O_4$ in 1 M Tris pH 10 was flushed through the flow cell. The resulting decrease in vesicle intensity due to quenching of the exterior NBD labels was recorded in the images.

Image Analysis. Images of immobilized vesicles were analyzed using an in-house written Matlab (Mathworks) program. Bright spots from immobilized vesicles were fitted to an asymmetric 2-dimensional Gaussian. The challenge of quantitatively analyzing intensity of a diffraction limited spot is usually[44−46] approached by fitting its intensity with a 2D-Gaussian function according to eq 1.

$$I(x,y) = b + A \times \exp\left\{-\left[\left(\frac{(x-x_0)}{r_x}\right)^2 + \left(\frac{(y-y_0)}{r_y}\right)^2\right]\right\} \quad (1)$$

Here, b is the background, A the amplitude, x and y are the image coordinates, (x_0,y_0) are the center of the fitted Gaussian function, and r_x and r_y are the $1/e$ widths in the two dimensions. However, the challenge of fitting vesicles in images was more complex. The spots are not diffraction limited due to their large size (up to several μm in diameter), therefore the orientation of the Gaussian function was considered as an additional parameter in the fit. This was accomplished by including a coordinate system rotation operator in the fitting program

$$\underline{R}_\alpha = \begin{bmatrix} \cos\alpha & \sin\alpha \\ -\sin\alpha & \cos\alpha \end{bmatrix} \quad (2)$$

in which α is the angle of rotation from the positive x-axis of the original coordinate system. The Gaussian equation modified to include α is

$$I(x,y) = b + A \times \exp\left\{-\left[\left(\frac{(x-x_0)\times\cos(\alpha)+(y-y_0)\times\sin(\alpha)}{r_x}\right)^2 + \left(\frac{(y-y_0)\times\cos(\alpha)+(x-x_0)\sin(\alpha)}{r_y}\right)^2\right]\right\} \quad (3)$$

The need for using a rotation-modified Gaussian to fit elongated vesicles is illustrated in Figure 2, where significant residual error between the fit and the data is observed when a simple 2-D fit is employed (see Figure 2E compared to 2C). Unlike the previous image analysis used for determining of vesicle intensities,[35] fitting the vesicle spots does not require selection of an intensity threshold, and it can analyze spots on a varying background within the same image. Additionally, the vesicles that are not spherically shaped can be included in the analysis, providing a more complete picture of the vesicle population.

From a fit of a measured spot to eq 3, the long- and short-axis radii of the intensity distribution can be determined, and the total intensity of the fitted spot was defined as the amplitude (A) multiplied by π times the product of the observed radii, r_x and r_y, in each dimension; these total intensities were used to evaluate lamellarity. After the measured radii in the image of the vesicles were determined, their sizes were corrected by deconvolution[47] to account for the Gaussian-shaped point spread function, where $r_{object}^2 = r_o^2 = r_{image}^2 - r_{psf}^2$. The surface areas of the vesicles are estimated from their mean-square radii, $SA \approx 4\pi(r_{x,o}^2 + r_{y,o}^2)/2$, where the average radius is given as a root-mean-square value $r_{avg} = [(r_{x,o}^2 + r_{y,o}^2)/2]^{1/2}$.

RESULTS AND DISCUSSION

The goal of this work is to characterize the distribution of both sizes and lamellarity of extruded vesicles by fluorescence imaging. Lamellarity can be assessed by quenching NBD on the outer leaflet of NBD-PE labeled vesicles by reaction with dithionite in the external solution.[29] This method was first applied on dispersion of NBD-PE labeled DPPC vesicles in bulk solution,

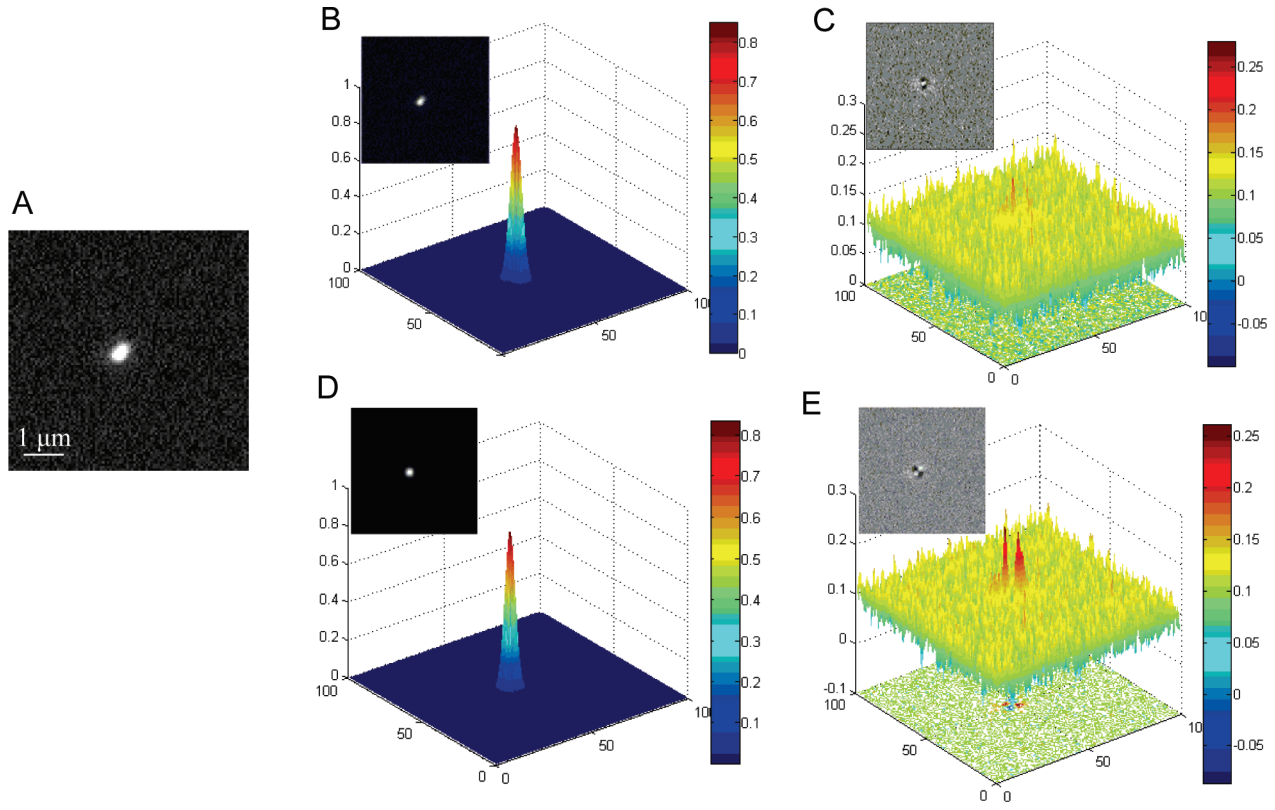

Figure 2. (A) Original image of skewed immobilized vesicle. B−E are the images and 3D contour plots including the following: (B) Fit of rotated 2-D Gaussian fit, with $\alpha = -54°$. (C) Residuals from rotated 2D-Gaussian fit. (D) Fit of 2-D Gaussian fit without rotation. (E) Residuals from 2D-Gaussian fit without rotation.

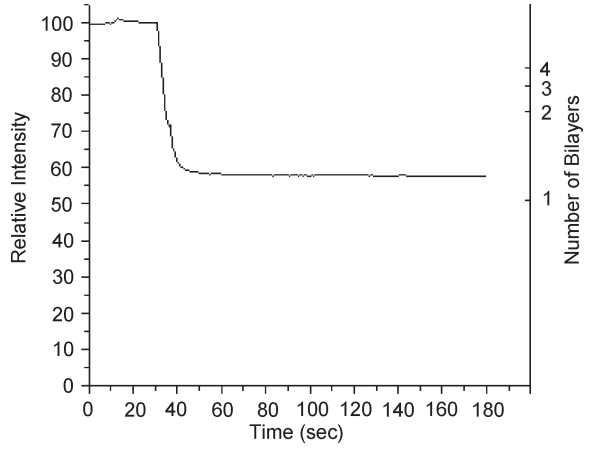

Figure 3. Plot of relative fluorescence from a population of DPPC vesicles showing fractional intensity loss as a result of quenching the outer bilayer leaflet. The remaining fluorescence due to lipid headgroup NBD-labels in the interior bilayers of the vesicles indicate that the vesicles in the population contain more than one bilayer.

producing a fractional loss of fluorescence intensity that can be interpreted to give the average number of lamellae present in the vesicle population; see Figure 3. Following quenching (and after correcting for dilution due to the volume of the quencher) the remaining intensity of unilamellar vesicles should be approximately 50% of the original measured intensity. The actual expected loss is slightly smaller due to the difference in areas of the outer and inner leaflet of the membrane, 49.5% for a 1 μm vesicle, assuming 0.48 nm^2 headgroup area and 5.1 nm bilayer thickness.[48] Similarly, the NBD residual intensity from vesicles with two concentric bilayers would be ~75% of the initial fluorescence intensity. The DPPC vesicles measured in bulk solution with a fluorimeter showed an average remaining intensity 60 ± 3% of the initial intensity, indicating the presence of multilamellar vesicles in the population. These average results do not indicate whether the multilamellar vesicles in the population are predominantly bilamellar vesicles, or if they represent more complex structures.

An analysis of the individual immobilized vesicles using fluorescence microscopy provides more insight into the composition of the population than a bulk dispersion experiment. Images of the immobilized vesicles before and after passing the dithionite quenching solution through the flow cell are shown in Figure 4. After analyzing the intensities of vesicles from images before and after the addition of dithionite, the NBD fluorescence quenching behavior of individual vesicles were plotted as a histogram, with average remaining intensity 65 ± 14% of the initial (Figure 5). It is apparent that some of the vesicles are unilamellar and many could be concentric bilamellar, but many vesicles show intermediate fractional losses of intensity. This is most likely caused by the presence of oligolamellar vesicles,[15,31] where smaller vesicles are encapsulated within a larger structure, for which only the exterior leaflet of the larger, surrounding vesicle is exposed to the quencher. This explanation is substantiated by the observation of a plot of the individual vesicle intensities versus their outer surface area estimated from their deconvoluted size in the image (Figure 6A). If the population

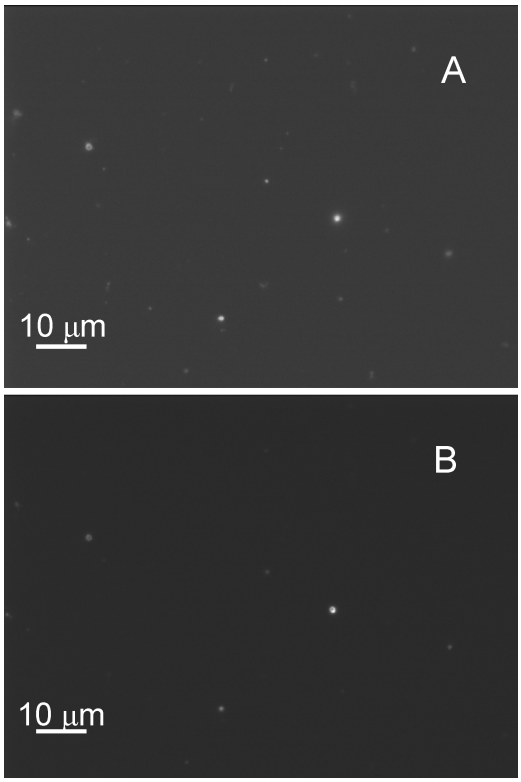

Figure 4. Images showing immobilized 1 μm extruded vesicles (A) before and (B) after quenching.

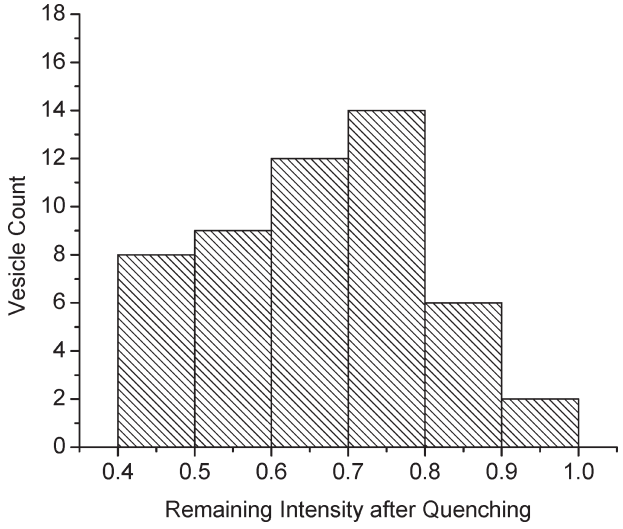

Figure 5. Histogram of relative vesicle intensities, indicating the distribution of unilamellar and multilamellar vesicles.

were composed only of unilamellar and concentric multilamellar vesicles, straight lines could be drawn through points from each population of vesicle lamellarity, where the intensity would scale with the outer surface area of the vesicle times the number of bilayers. For example, bilamellar vesicles would fall on a line with a slope of twice the slope of the line for unilamellar vesicles. Evidence of this trend can be observed in a fraction of the population by plotting total intensity versus outer surface area for vesicles whose dithionite-quenching behavior indicated they

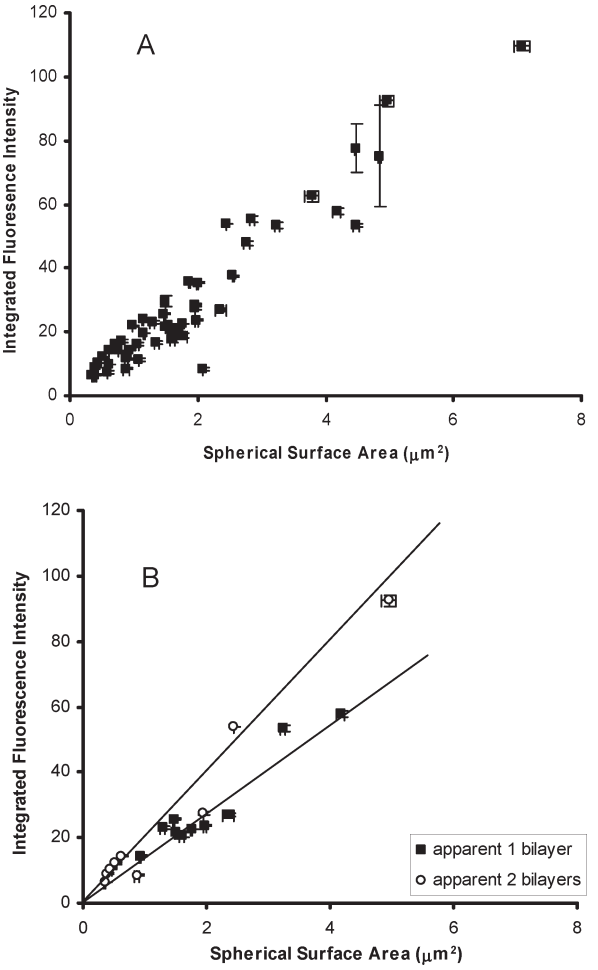

Figure 6. (A) Plot of vesicle intensity with surface area for all 1 μm extruded DPPC vesicles. (B) Vesicles sorted by relative quenched intensity that indicate they are unilamellar (dark squares, slope 13 $\pm$ 2) or bilamellar (open circles, slope = 19 $\pm$ 2).

were unilamellar (fractional intensity loss between 0.45 and 0.55) and concentric bilamellar (loss between 0.70 and 0.80); see Figure 6B. Within the large uncertainties in the slopes of these lines, unilamellar (13 $\pm$ 2) and bilamellar (19 $\pm$ 2), the upper bound of the ratio of the two slopes relating intensity and area (1.9) is close to the expected factor two. For the entire population, however, the nearly continuous fractional intensity changes upon quenching and absence of a linear dependence between fluorescence intensity and outer surface area are indicative of a significant fraction of oligolamellar vesicles.

Imaging immobilized vesicles also provides information about the vesicle size distribution. Since extrusion of vesicles through pores of known size is employed for size selection, we examined the vesicle radius reported from the Gaussian fit of the vesicle spots (corrected for the point spread function). Since the vesicles were extruded using 1 μm polycarbonate membrane pores, it was expected that the majority of vesicles would be less than the diameter of the pores. As shown in the histogram of vesicle radii plotted in Figure 7, many vesicles are produced at $\sim$1-μm diameter, but with a wide distribution around an average diameter of 0.8 $\pm$ 0.2 μm.

To test the validity of the quenching method applied to characterizing images of single vesicles, a control sample of

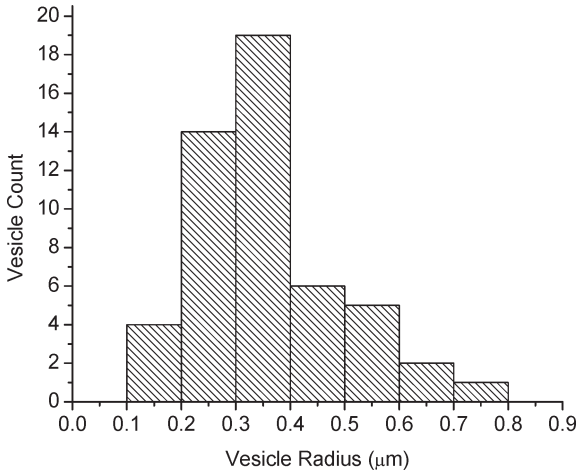

Figure 7. Histogram of vesicle radius distribution for 1-μm diameter extruded DPPC vesicles.

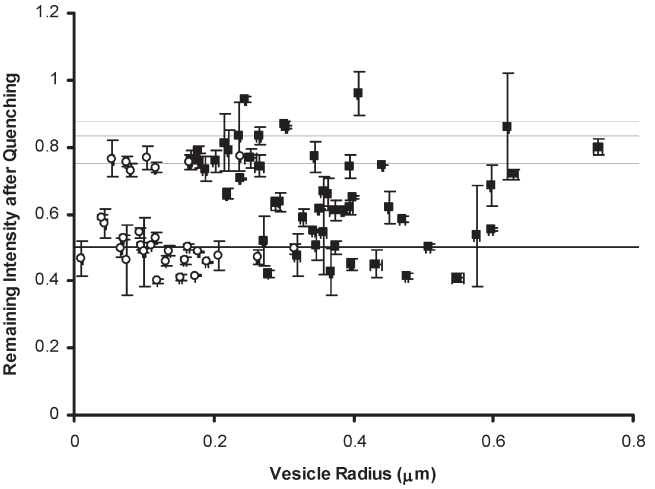

Figure 8. Plot of vesicle radius and relative remaining intensity after quenching for both 1-μm (filled squares) extruded vesicles and 100-nm (open circles) freeze−thaw extruded vesicles. Radii of vesicles are deconvoluted with the microscope point spread function.

smaller vesicles was prepared using procedures that have been reported to produce a more unilamellar vesicle population.[22] This sample was prepared by first subjecting the hydrated lipid solution to 5 freeze−thaw cycles followed by extrusion through two stacked membranes with 100-nm pores. When the fractional remaining intensity was calculated for several of the imaged 100-nm vesicles, two populations of vesicles emerged: those quenched to approximately 50%, and a smaller number quenched to approximately 75% of their initial intensity. The results plotted in Figure 8 (open circles) show that these vesicles were predominantly unilamellar, with fewer bilamellar vesicles present. Oligolamellar vesicles were not nearly as prevalent for the 100-nm vesicles as they were for the 1-μm extruded vesicles, as shown for comparison in Figure 8 (filled squares).

It is important to scrutinize the assumptions of this quenching method to assess the validity of their interpretation. The assumption that the SO_2^- quencher ion does not permeate the DPPC bilayer is supported by the impermeability of the DPPC bilayers to perchlorate ion, as described by Cherney and co-workers,[24] who used confocal Raman microscopy to test vesicles prepared from various lipids for their perchlorate ion-permeability. In that study, DPPC vesicles were shown to retain perchlorate without leakage to the vesicle exterior for over 6 h. Further evidence can be found in the results reported here, where the fluorescence intensity after quenching reaches a plateau with residual intensity following the addition of the quencher (see Figure 3). These results indicate that the membranes do not have defects that would lead to a slow transport of dithionite into the vesicle interior.

Another assumption that should be examined is the probability that lipid flip-flop (the movement of a lipid from the inner leaflet of the bilayer to the exterior leaflet) does not occur throughout the duration of the quenching experiment (for the bulk experiment, 180 s). If flip-flop of the NBD-PE occurred rapidly, the interior labels could be exposed to the quencher in the exterior solution. The kinetics of lipid flip-flop have been recently investigated, and the flip-flop rate for DPPC planar lipid bilayers near room temperature cast at a surface pressure of 30 mN/m is reported to be 3.95×10^{-5} s^{-1}.[49] This indicates that the probability of a DPPC flip-flop event is only 0.007 over the 180-s course of the experiment. The modification of the lipid headgroup with a headgroup label slows the flip-flop rate even further, as much as an order of magnitude,[49] such that the NBD-PE lipid would undergo even fewer flip-flop events than DPPC. This is consistent with the observation that the fluorescence intensity in the bulk experiment decreases initially with addition of the quencher, and then levels off to a steady final intensity. It can therefore be concluded that lipid flip-flop does not interfere on the time-scale of the measurement. If it had, a gradual decrease in intensity would be observed at the rate equal to that of the labeled lipids on the interior leaflet moving to the exterior of the vesicle.

CONCLUSIONS

A method for the immobilization, imaging, and quantitative analysis of the size and lamellarity of individual vesicles in parallel was described. The surface modification of a glass coverslip with silane-bound biotin tethers allowed the formation of a biotin−avidin-biotin conjugate to immobilize biotinylated vesicles; these immobilized vesicles could be observed over long times and imaged under flowing solution conditions. The vesicle fluorescence images were fit to two-dimensional Gaussian functions and deconvoluted, to account for the point-spread function of the microscope, producing size distributions that included vesicles with nonspherical shapes. Fluorescence images before and after quenching of the outer-leaflet fluorescence label enabled the evaluation of the corresponding lamellarity of individual vesicles. The results showed a distribution of vesicle sizes, produced by extrusion, in a diverse population that contains unilamellar, multilamellar, and oligolamellar structures. This method of analysis should be useful in research that relies on vesicles of controlled size or lamellarity.

AUTHOR INFORMATION

Corresponding Author

*E-mail: harrisj@chem.utah.edu.

Present Addresses

[†] Institut für Physikalische und Theoretische Chemie, TU Braunschweig, 38106 Braunschweig, Germany.

■ ACKNOWLEDGMENT

This research was supported in part by the National Science Foundation under Grant CHE-0957242.

■ REFERENCES

(1) Hong, M.; Weekley, B. S.; Grieb, S. J.; Foley, J. P. *Anal. Chem.* **1998**, *70*, 1394–1403.
(2) Cunliffe, J. M.; Baryla, N. E.; Lucy, C. A. *Anal. Chem.* **2002**, *74*, 776–783.
(3) Wang, C.; Lucy, C. A. *Anal. Chem.* **2005**, *77*, 2015–2021.
(4) Drummond, D. C.; Zignani, M.; Leroux, J.-C. *Prog. Lipid Res.* **2000**, *39*, 409–460.
(5) Samad, A.; Sultana, Y.; Aqil, M. *Curr. Drug Delivery* **2007**, *4*, 297–305.
(6) Roberts, D. L.; Ma, Y.; Bowles, S. E.; Janczak, C. M.; Pyun, J.; Saavedra, S. S.; Aspinwall, C. A. *Langmuir* **2009**, *25*, 1908–1910.
(7) Chiu, D. T.; Wilson, C. F.; Ryttsen, F.; Stromberg, A.; Farre, C.; Karlsson, A.; Nordholm, S.; Gaggar, A.; Modi, B. P.; Moscho, A.; Garza-Lopez, R. A.; Orwar, O.; Zare, R. N. *Science* **1999**, *283*, 1892–1895.
(8) Walde, P.; Ichikawa, S. *Biomol. Eng.* **2001**, *18*, 143–177.
(9) Okumus, B.; Wilson, T. J.; Lilley, D. M.; Ha, T. *Biophys. J.* **2004**, *87*, 2798–2806.
(10) Michel, M.; Winterhalter, M.; Darbois, L.; Hemmerle, J.; Voegel, J. C.; Schaaf, P.; Ball, V. *Langmuir* **2004**, *20*, 6127–6133.
(11) Yang, T.; Jung, S.-y.; Mao, H.; Cremer, P. S. *Anal. Chem.* **2001**, *73*, 165–169.
(12) Cheng, Z.; Aspinwall, C. A. *Analyst* **2006**, *131*, 236–243.
(13) Edwards, K. A.; Baeumner, A. J. *Talanta* **2006**, *68*, 1421–1431.
(14) Moscho, A.; Orwar, O.; Chiu, D. T.; Modi, B. P.; Zare, R. N. *Proc. Natl Acad. Sci. U.S.A.* **1996**, *93*, 11443–11447.
(15) Mui, B.; Chow, L.; Hope, M. J. *Methods Enzymol.* **2003**, *367*, 3–14.
(16) Akashi, K.-i.; Miyata, H.; Itoh, H.; Kazuhiko Kinosita, J. *Biophys. J.* **1998**, *74*, 2973–2982.
(17) Hope, M. J.; Bally, M. B.; Webb, G.; Cullis, P. R. *Biochim. Biophys. Acta* **1985**, *812*, 55–65.
(18) Barenholz, Y.; Gibbes, D.; Litman, B. J.; Goll, J.; Thomson, T. E.; Carlson, F. D. *Biochemistry* **1977**, *16*, 2806–2810.
(19) Castile, J. D.; Taylor, K. M. G. *Int. J. Pharm.* **1999**, *188*, 87–95.
(20) MacDonald, R. C.; MacDonald, R. I.; Menco, B. P. M.; Takeshita, K.; Subbarao, N. K.; Hu, L.-r. *Biochim. Biophys. Acta* **1991**, *1061*, 297–303.
(21) Schmiedel, H.; Almásy, L.; Klose, G. *Eur Biophys J* **2006**, *35*, 181–189.
(22) Mayer, L. D.; Hope, M. J.; Cullis, P. R. *Biochim. Biophys. Acta* **1986**, *858*, 161–168.
(23) Fox, C. B.; Uibel, R. H.; Harris, J. M. *J. Phys. Chem. B* **2007**, *111*, 11428–11436.
(24) Cherney, D. P.; Conboy, J. C.; Harris, J. M. *Anal. Chem.* **2003**, *75*, 6621–6628.
(25) Fox, C. B.; Horton, R. C.; Harris, J. M. *Anal. Chem.* **2006**, *78*, 4918–4924.
(26) Long, M. S.; Jones, C. D.; Helfrich, M. R.; Mangeney-Slavin, L. K.; Keating, C. D. *Proc. Natl Acad. Sci. U.S.A.* **2005**, *102*, 5920–5925.
(27) Hsin, T.-M.; Yeung, E. S. *Angew. Chem., Int. Ed.* **2007**, *43*, 8032–8035.
(28) Engelhaaf, S. U.; Wehrli, B.; Müller, M.; Adrian, M.; Schurtenberger, P. *J. Microsc.* **1996**, *184*, 214–228.
(29) McIntyre, J. C.; Sleight, R. G. *Biochemistry* **1991**, *30*, 11819–11827.
(30) Sato, K.; Obinata, K.; Sugawara, T.; Urabe, I.; Yomo, T. *J. Biosci. Bioeng.* **2006**, *102*, 171–178.
(31) Bagatolli, L. A.; Parasassi, T.; Gratton, E. *Chem. Phys. Lipids* **2000**, *105*, 135–147.
(32) Maestrelli, F.; González-Rodríguez, M. L.; Rabasco, A. M.; Mura, P. *Int. J. Phramaceutics* **2006**, *312*, 53–60.
(33) Givan, A. L. *Flow Cytometry First Principles*; Wiley-Liss, Inc.: New York, 1992.
(34) Vorauer-Uhl, K.; Wagner, A.; Borth, N.; Katinger, H. *Cytometry* **2000**, *39*, 166–171.
(35) Lohr, C.; Kunding, A. H.; Bhatia, V. K.; Stamou, D. *Methods Enzymol.* **2009**, *465*, 143–160.
(36) Wasmuth, C. R.; Edwards, C.; Hutcherson, R. *J. Phys. Chem.* **1964**, *68*, 423–425.
(37) Wayment, J. R.; Harris, J. M. *Anal. Chem.* **2006**, *78*, 7841–7849.
(38) Jung, L. S.; Shumaker-Parry, J. S.; Campbell, C. T.; Yee, S. S.; Gelb, M. H. *J. Am. Chem. Soc.* **2000**, *122*, 4177–4184.
(39) Boukobza, E.; Sonnenfeld, A.; Haran, G. *J. Phys. Chem. B* **2001**, *105*, 12165–12170.
(40) Charles, P. T.; Conrad, D. W.; Jacobs, M. S.; Bart, J. C.; Kusterbeck, A. W. *Bioconjug. Chem.* **2002**, *6*, 691–694.
(41) Houlne, M. P.; Sjostrom, C. M.; Uibel, R. H.; Kleimeyer, J. A.; Harris, J. M. *Anal. Chem.* **2002**, *74*, 4311–4319.
(42) Hanley, D. C.; Harris, J. M. *Anal. Chem.* **2001**, *73*, 5030–5037.
(43) Heider, E. C.; Barhoum, M.; Peterson, E. M.; Schaefer, J.; Harris, J. M. *Appl. Spectrosc.* **2010**, *64*, 37–45.
(44) Kiessling, V.; Crane, J. M.; Tamm, L. K. *Biophys. J.* **2006**, *91*, 3313–3326.
(45) Schütz, G. J.; Schindler, H.; Schmidt, T. *Biophys. J.* **1997**, *73*, 1073–1080.
(46) McCain, K. S.; Hanley, D. C.; Harris, J. M. *Anal. Chem.* **2003**, *75*, 4351–4359.
(47) Bracewell, R. N. *The Fourier Transform and Its Applications*; McGraw-Hill: New York, 1986.
(48) Cevc, G.; Marsh, D. *Phospholipid Bilayers: Physical Principles and Models*; John Wiley & Sons: New York, 1987.
(49) Liu, J.; Conboy, J. C. *Biophys. J.* **2005**, *89*, 2522–2532.